Iron Chelators of the Dipyridylketone Thiosemicarbazone Class: Precomplexation and Transmetalation Effects on Anticancer Activity

Paul V. Bernhardt,*[,§] Philip C. Sharpe,[§] Mohammad Islam,[§] David B. Lovejoy,[‡] Danuta S. Kalinowski,[‡] and Des R. Richardson*[,‡]

Centre for Metals in Biology, School of Chemistry and Molecular Biosciences, University of Queensland, Brisbane, Qld 4072, Australia, and Department of Pathology and Bosch Institute, University of Sydney, Sydney, NSW 2006, Australia

Received August 12, 2008

We previously reported a series of di-2-pyridylketone thiosemicarbazone (**H**DpT) chelators that showed marked and selective antitumor activity (Whitnall, M.; *et al. Proc. Natl. Acad. Sci. U.S.A.* **2006**, *103*, 14901−14906). To further understand their biological efficacy, we report the characterization and activity of their Mn^{II}, Co^{III}, Ni^{II}, Cu^{II}, and Zn^{II} complexes. The X-ray crystal structures of four divalent (Mn, Ni, Cu, and Zn) and one trivalent (Fe) complexes are reported. Electrochemistry shows the $Fe^{III/II}$ and $Cu^{II/I}$ potentials of the complexes may be redox-active within cells. Stability constants were also determined for the Mn^{II}, Ni^{II}, Cu^{II}, and Zn^{II} complexes. All divalent complexes underwent transmetalation upon encountering Fe^{II}, to form low spin ferrous complexes. Importantly, the divalent Mn^{II}, Ni^{II}, Cu^{II}, and Zn^{II} complexes of the **H**DpT analogues are equally active in preventing proliferation as their ligands, suggesting the complexes act as lipophilic vehicles facilitating intracellular delivery of the free ligand upon metal dissociation.

Introduction

The search for novel compounds that are able to prevent cancer cell proliferation is ongoing, as many current chemotherapies remain ineffective against common and aggressive tumors, e.g., malignant melanoma and breast, prostate, lung, and brain cancer. Another major problem is the resistance of certain cancers to traditional chemotherapeutics, many of which target DNA. This challenge calls for new strategies and drugs that take advantage of novel molecular targets that are key components of cellular metabolism and replication.

Recent work by our group and others in this area has focused on the essential nutrient iron (Fe). This has been achieved by developing specific Fe chelators that markedly inhibit tumor cell growth in vitro and in vivo.[1−7] In fact, a number of animal studies and clinical trials with the thiosemicarbazone Triapine (3-amino-2-pyridinecarbaldehyde thiosemicarbazone, Chart 1) have demonstrated that this strategy is clearly promising.[8−10]

Iron is crucial for many metabolic reactions including the rate-limiting step of DNA synthesis involving the Fe-dependent enzyme, ribonucleotide reductase (RR[a]), which converts ribonucleotides to deoxyribonucleotides.[11,12] However, this is not the only target, with molecules linked to events such as cell cycle control and metastasis suppression also being implicated.[11,13,14] In all cases that have been investigated, the antiproliferative activity of the ligands has been correlated, at least to some extent, with their ability to chelate intracellular Fe.[2,4,15,16]

The compounds we have investigated to date are all tridentate chelators of the hydrazone (**H**PKIH,[1] $\mathbf{H}_2$NIH[17]), thiosemicarbazone (**H**DpT[2,4,16,18]), or thiohydrazone (**H**PKTBH[3]) classes, and representative examples are given in Chart 1. Each compound forms well characterized six-coordinate 1:2 Fe/ligand complexes. The preferred oxidation state of the metal is very much dependent on the donor atoms present. The N,N,O chelators that we have studied[1,19−21] (Chart 1, donor atoms highlighted in bold type) are specific for Fe^{II}, while the O,N,O hydrazones are Fe^{III} chelators.[17] The introduction of S-donors renders the thiosemicarbazone and thiohydrazone ligands capable of supporting Fe in either oxidation state. This has been established synthetically by isolation of both di- and trivalent Fe complexes[2] and supported by reversible electrochemistry at potentials accessible to biological oxidants and reductants.[3,4] Indeed, the pronounced antitumor activity of some of the **H**DpT analogues (e.g., **H**Dp44mT, Chart 2) is mediated by the proposed "double punch" mechanism.[2,22] This is characterized by their ability to bind cellular Fe (the first punch) to form redox-active Fe complexes (the second punch) that leads to marked and selective anticancer activity.[16,18] The Fe complexes of the **H**DpT analogues exhibit significant, although typically lower, antiproliferative activity compared with their metal-free ligands.[2,4]

While the resupply of Fe to the tumor *in vivo* could dampen the antitumor effects of chelators, there are several considerations that suggest that this is not effective. Indeed, apart from data showing the effectiveness of other chelators in clinical trials,[12] we demonstrated using tumor xenografts in nude mice that certain **H**Dpt analogues effectively inhibit tumor growth.[16,18] Moreover, an important mode of cytotoxicity of the agents is their ability to form redox-active Fe complexes, and thus, the resupply of Fe to the tumor *in vivo* probably does not allow effective rescue.

* To whom correspondence should be addressed. For P.V.B.: phone, +61-7-3365-4266; fax, +61-7-3365-4299; e-mail, p.bernhardt@uq.edu.au. For D.R.R.: phone, +61-2-9036-6548; fax, +61-2-9351-3429; e-mail, d.richardson@med.usyd.edu.au.

§ University of Queensland.

‡ University of Sydney.

[a] Abbreviations: RR, ribonucleotide reductase; DFO, desferrioxamine B; **H**PKIH, dipyridylketone isonicotinoyl hydrazone; $\mathbf{H}_2$NIH, 2-hydroxy-1-naphthaldehyde isonicotinoyl hydrazone; **H**DpT, dipyridylketone thiosemicarbazone, **H**PKTBH, dipyridylketone thiobenzoylhydrazone; **H**Dp44mT, dipyridylketone 4,4-dimethylthiosemicarbazone; **H**Dp4mT, dipyridylketone 4-methylthiosemicarbazone; **H**Dp4eT, dipyridylketone 4-ethylthiosemicarbazone; **H**Dp4pT, dipyridylketone 4-phenylthiosemicarbazone; **H**Dp4aT, dipyridylketone 4-allylthiosemicarbazone; DMSO, dimethyl sulfoxide; MeCN, acetonitrile; DMF, dimethylformamide; MLCT, metal to ligand charge transfer; EPR, electron paramagnetic resonance; NHE, normal hydrogen electrode; H_3NTA, nitrilotriacetic acid; H_4EDTA, ethylenediaminetetraacetic acid; H_5DTPA, diethylenetriaminepentaacetic acid; Tf, transferrin.

10.1021/jm801012z CCC: $40.75
Published on Web 12/17/2008

Chart 1

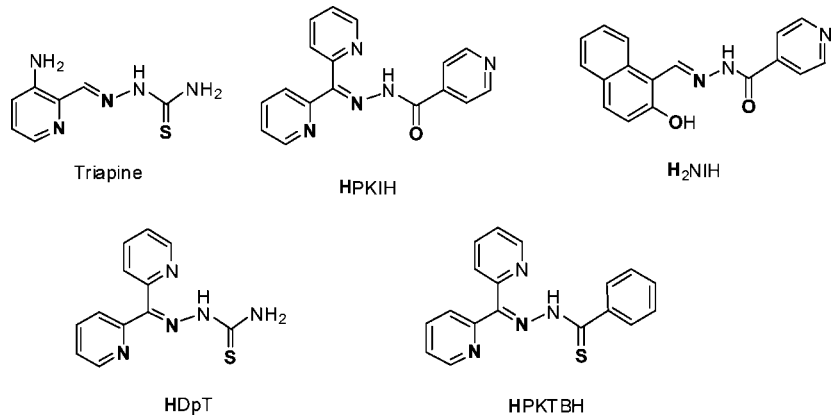

Chart 2

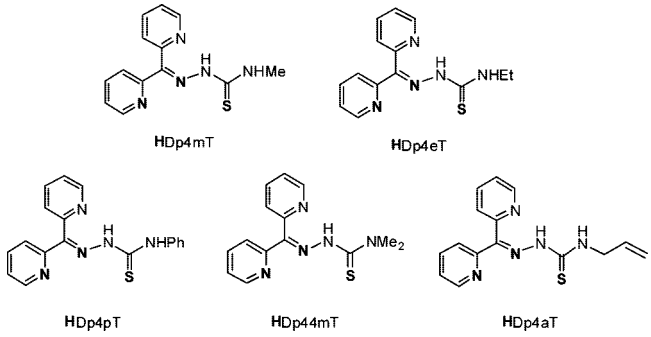

Although intracellular Fe chelation by these tridentate metal-free ligands appears to be an important part of their mode of action, we have shown that this alone cannot explain the antiproliferative activities of these compounds. In particular, precomplexation of **H**PKIH (Chart 1) with the divalent Mn, Fe, Co, Ni, Cu, and Zn ions generated compounds that still exhibited significant antiproliferative activity.[23] No obvious explanation for this preservation of anticancer activity despite precomplexation has emerged. However, we have speculated it may be related to dissociation of the complexes within the cell to release the more active free ligand or potentially related to transmetalation upon encountering intracellular Fe.[23]

Herein, we report the characterization and biological activity of the Mn, Fe, Co, Ni, Cu, and Zn complexes of the **H**DpT analogues, many of which show marked antitumor activity *in vitro*. We demonstrate that the divalent complexes of these ligands are equally able to prevent cellular proliferation as the free ligands, and we show that the complexes are indeed able to undergo transmetalation in the presence of Fe^{II}. In the presence of air, all Fe complexes oxidize to their ferric form, and we show that these complexes are particularly stable. This study is important for further understanding the unusually pronounced biological activity of these ligands.

Results and Discussion

Syntheses and Spectroscopy. The syntheses of all complexes were straightforward and high yielding. The compounds were only sparingly soluble in water but exhibit greater solubility in polar organic solvents such as DMSO, MeCN, and DMF. In most cases, divalent complexes were formed of the formula ML_2 (where the ligand is singly deprotonated). The Co^{III} analogues were the exception, being isolated in their trivalent form after spontaneous oxidation of the Co^{II} analogue during preparation. As reported previously,[2] the Fe complexes of the **H**DpT analogues may be obtained in their divalent forms from a ferrous salt precursor under anaerobic conditions or in their trivalent forms using ferric salts.

The electronic spectra of all complexes are dominated by intense transitions in the UV region that tail into the visible region, giving most complexes a dark-brown color. The Fe^{II} complexes are different and are characteristically blue-green, each showing an intense MLCT transition around 650 nm. The Zn^{II} complexes are bright-yellow, lacking any electronic transitions involving d electrons and also exhibiting much higher energy ligand based absorption bands that barely enter the visible region of the spectrum.

Structural Characterization. In support of other characterization data, the X-ray crystal structures of four divalent complexes of the **H**DpT analogues $[Mn(Dp4pT)_2]\cdot DMF$, $[Ni(Dp4pT)_2]\cdot {}^1/_2MeCN\cdot {}^1/_2H_2O$, $Cu(Dp44mT)_2$, and $Zn(Dp4mT)_2$ were determined in addition to the trivalent complex $[Fe(DpT)_2](ClO_4)$. A view of each complex is shown in Figure 1. Despite the similar metal−ligand stoichiometry, the structures are distinctly different and reflect the preferences of each metal ion. The Mn^{II} complex exhibits a highly distorted and irregular six-coordinate geometry by comparison with its Ni^{II} and Zn^{II} analogues. The ideally linear N3a−M−N3b coordinate angle is ∼153° in the Mn^{II} complex compared with ∼162° (Zn) and ∼176° (Ni) (Table 2). A molecule of DMF accepts an H-bond from an −NHPh group (N5a) in the Mn complex (not shown) which may be related to the distorted geometry we observe. This is suggested, as a related[24] thiosemicarbazone complex of Mn^{II} (bearing a terminal pyrrolidine group rather than a phenyl ring) exhibits a very similar coordination geometry to $Mn(Dp4pT)_2$, despite a different lattice structure and no solvent of crystallization.

The Ni^{II} structure comprises two complexes in the asymmetric unit exhibiting similar conformations. The main difference between the two molecules is that the phenyl ring is disordered between two positions in one of the ligands while the other complex is ordered. Interestingly, this structure is isomorphous with that reported for $[Ni(Dp4pT)_2]\cdot {}^1/_2DMF\cdot {}^1/_2H_2O$,[25] where the DMF molecule can be substituted for MeCN with retention of the same structure.

The coordinate bonds follow expected trends on the basis of their d-electron configurations and position in the first transition series (Mn^{II} (d^5) > Ni^{II} (d^8) > Cu^{II} (d^9) < Zn^{II} (d^{10})), a trend consistent with the Irving−Williams order.[26] The rigid and ideally planar ligands enforce consecutive, meridionally disposed five-membered chelate rings. Distortions of the coordinate angles within each chelate ring (ideally ∼80−85°) are correlated with the coordinate bond lengths. As the coordinate bonds become

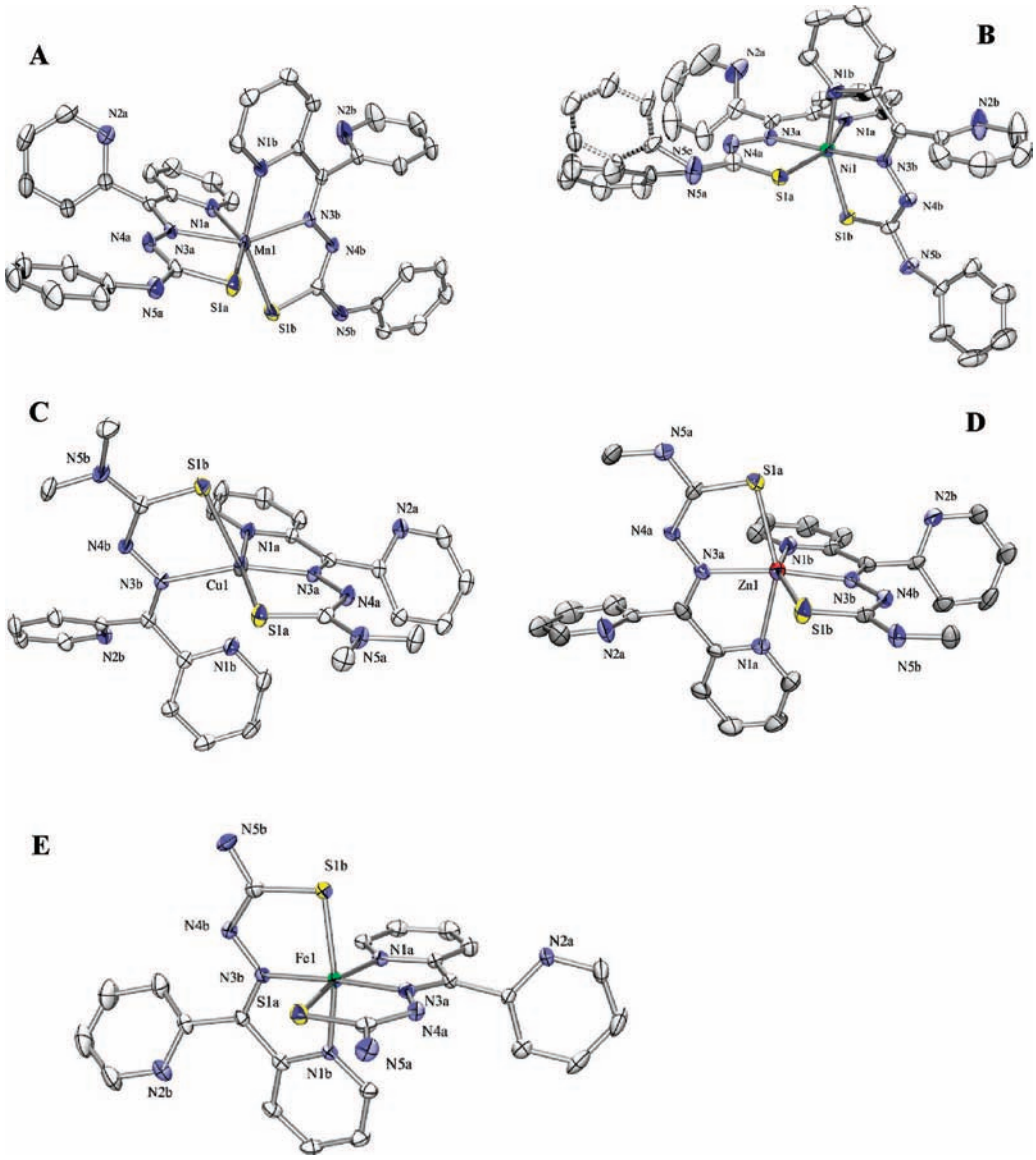

Figure 1. ORTEP views (30% probability ellipsoids, H-atoms omitted) of (A) $Mn(Dp4pT)_2$, (B) $Ni(Dp4pT)_2$ (showing phenyl ring disorder in molecule 1), (C) $Cu(Dp44mT)_2$, (D) $Zn(Dp4mT)_2$, and (E) $[Fe(DpT)_2]^+$ (counteranion omitted).

Table 1. Crystal Data

	$[Mn(Dp4pT)_2]\cdot$ DMF	$[Fe(DpT)_2]ClO_4$	$[Ni(Dp4pT)_2]\cdot{}^1/_2$ $MeCN\cdot{}^1/_2H_2O$	$Cu(Dp44mT)_2$	$Zn(Dp4mT)_2$
formula	$C_{39}H_{35}MnN_{11}OS_2$	$C_{24}H_{20}ClFeN_{10}O_4S_2$	$C_{37}H_{30.5}N_{10.5}NiO_{0.5}S_2$	$C_{28}H_{28}CuN_{10}S_2$	$C_{26}H_{24}N_{10}S_2Zn$
formula weight	792.84	667.92	753.05	632.26	606.04
crystal system	triclinic	monoclinic	monoclinic	monoclinic	monoclinic
space group	$P\bar{1}$ (No. 2)	$P2_1/n$ (No. 14)[a]	$P2_1/n$ (No. 14)[a]	$P2_1/c$ (No. 14)	$P2_1/n$ (No. 14)[a]
color	dark-brown	black	dark-brown	dark-brown	yellow
a, Å	10.897(2)	13.3578(5)	15.072(1)	10.0347(9)	10.7273(9)
b, Å	12.246(3)	15.9553(5)	28.678(1)	19.770(2)	15.224(2)
c, Å	14.898(2)	13.8014(5)	17.321(1)	14.461(2)	17.276(4)
α, deg	85.01(2)				
β, deg	73.28(1)	108.511(4)	105.607(7)	97.53(1)	90.69(1)
γ, deg	79.93(2)				
V, Å^3	1873.3(6)	2789.3(2)	7210.6(7)	2844.1(6)	2821.2(8)
T, K	293	293	293	293	293
Z	2	4	8	4	4
R1 (obsd data)	0.0680	0.0421	0.0528	0.0413	0.0576
wR2 (all data)	0.2261	0.0967	0.1006	0.1155	0.1586
GOF	1.029	0.940	0.727	1.009	0.971
CCDC	698 207	698 208	698 209	698 210	698 211

[a] Variant of $P2_1/c$.

longer, the inflexible ligand maintains the same conformation, leading to a contraction of the coordinate angles. A similar feature is seen in contraction of the *trans* N1a,b−M−S1a,b angles away from linearity as the metal ion becomes larger.

Table 2. Selected Bond Lengths (Å) and Angles (deg)

	$[Mn(Dp4pT)_2]\cdot$ DMF	$[Fe(DpT)_2](ClO_4)$	$[Ni(Dp4pT)_2]\cdot {}^1/_2MeCN\cdot {}^1/_2H_2O$[a]	$Cu(Dp44mT)_2$	$Zn(Dp4mT)_2$
M−N1a, M−N1b	2.256(5), 2.295(5)	1.969(3), 1.979(3)	2.083(4), 2.115(5)	2.042(3), 2.495(3)	2.252(6), 2.214(6)
M−N3a, M−N3b	2.274(4), 2.252(4)	1.915(2), 1.921(2)	2.029(5), 2.010(5)	2.005(3), 2.177(3)	2.134(6), 2.138(5)
M−S1a, M−S1b	2.500(2), 2.526(2)	2.226(1), 2.229(1)	2.373(2), 2.443(2)	2.308(1), 2.476(1)	2.501(2), 2.414(2)
N1a−M−N1b	88.7(2)	87.7(1)	89.7(2)	83.5(1)	85.9(2)
N3a−M−N3b	153.1(2)	174.8(1)	175.8(2)	157.3(1)	161.3(2)
S1a−M−S1b	97.46(7)	95.53(4)	98.88(6)	95.46(4)	102.39(8)
S1a−M−N1a	146.5(1)	166.32(7)	158.95(17)	161.89(9)	152.9(2)
S1a−M−N3a	75.9(1)	81.6(1)	81.4(2)	82.84(9)	74.7(2)

[a] Molecule 1.

The ferric complex $[Fe(DpT)_2](ClO_4)$ exhibits the shortest coordinate bond lengths (Table 2) of this series, and these are consistent with a low spin d^5 electronic ground state. The bond lengths are also typical of Fe^{III} heterocyclic thiosemicarbazone complexes.[27−30] In an earlier paper,[4] we reported the crystal structure of the Fe^{II} complex of a closely related 3-nitrophenylpyridyl thiosemicarbazone where a low spin (d^6) complex was also identified in the solid state. This Fe^{II} complex exhibits coordinate bonds that are almost the same as those found here for the Fe^{III} analogue. It is apparent that all of the ferric and ferrous complexes of the **H**DpT analogues are low spin. This point is of considerable importance to the relative stabilities of Fe complexes relative to other metal complexes reported here.

A distinguishing feature of the Cu^{II} structure is its asymmetry. Unlike the Fe^{III}, Mn^{II}, Ni^{II}, and Zn^{II} structures, where the pairs of corresponding coordinate bond lengths to the two ligands are more or less the same, the two ligands bonded to Cu (denoted with "a" and "b" labels) are distinct. Ligand "a" forms Cu−N and Cu−S bond lengths that are consistently shorter than those to ligand "b". The explanation for this lies in the electronic ground state of the Cu ion (d^9) where an axial elongation (along N1b−Cu−S1b) is apparent, resulting in a pronounced splitting of the e_g (d_{z^2} and $d_{x^2-y^2}$) set of orbitals (Jahn−Teller effect). This distortion forcing S1b and N1b away from the Cu ion is so large that the Cu−N3b bond is also weakened. The fact that the Cu−S1b bond is shorter than Cu−N1b (despite the larger S-atom covalent radius) indicates that the complex is better described as five-coordinate, with N1b being outside the coordination sphere. All Cu complexes were isolated in a 1:2 metal/ligand ratio. It is relevant that heterocyclic thiosemicarbazone coordination compounds of Cu^{II} are commonly found to be 1:1 (CuL) and 2:2 (Cu_2L_2) complexes, the latter involving an S-bridged dimeric structure where the thiosemicarbazone forms a strong equatorial coordinate bond while also binding weakly in the axial coordinate site of an adjacent Cu center.[31−35]

In support of crystallographic characterization, the EPR spectra of the Cu^{II} complexes were measured in dilute frozen solutions. The spin Hamiltonian parameters determined by spectral simulation (Supporting Information, Figure S1) are characteristic of an axially elongated coordination sphere with an additional rhombic distortion, i.e. g_z (A_z) ≫ g_y (A_y) ∼ g_x (A_x). The *g* and *A* values show similar trends as reported earlier for Cu^{II} complexes of related hydrazone ligands.[19,23] An illustrative example is given in Figure 2 for $Cu(Dp4pT)_2$. The EPR spectra, although similar, do reveal subtle differences across the six different Cu complexes in their spin Hamiltonian parameters, most importantly in the magnitude of A_z. This decreases with distortions of the coordinate angles from ideal values (90°, 180°) and rhombic distortions ($g_z > g_y > g_x$). These structural variations are presumably due to steric effects of the noncoordinating alkyl, aryl, and allyl substitutents on the terminal N-atom. Because the EPR measurements were made on dilute solutions, they are truly representative of variations in molecular structure and unaffected by intermolecular interactions of the type seen in the solid state crystallographically derived structures.

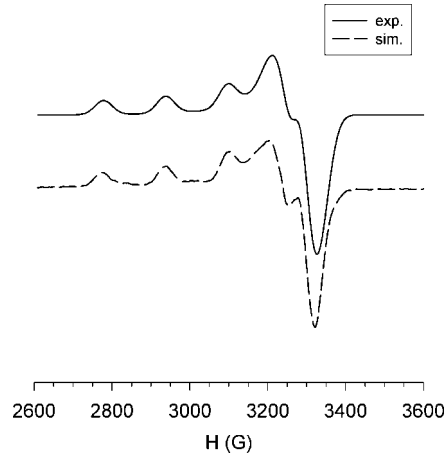

Figure 2. Experimental (solid line) and simulated (broken line) EPR spectra of $Cu(Dp4pT)_2$ (1 mM DMF/H_2O 2:1, 77 K). Spin Hamiltonian parameters used to generate simulated spectrum were as follows: g_x = 2.037 (A_x = 19 G), g_y = 2.057 (A_y = 12 G), g_z = 2.202 (A_z = 159 G).

Table 3. Redox Potentials (mV vs NHE) Measured in 70% Aqueous MeCN

ligand (HL)	complex				
	$Mn^{III/II}L_2$	$Fe^{III/II}L_2$	$Co^{III/II}L_2$	$Ni^{III/II}L_2$	$Cu^{II/I}L_2$
HDpT	+542 (irrev)	+165	−525	+620	−72 (irrev)
HDp4mT	+454	+153	−570	+573	−64 (irrev)
HDp4eT	+465 (irrev)	+166	−579	+568	−61 (irrev)
HDp44mT	+387	+173	−623	+524	−210
HDp4pT	+514	+225	−503	+617	−100
HDp4aT	+461 (irrev)	+170	−559	+582	−23

Electrochemistry. All complexes, except for those with Zn^{II}, exhibited single electron metal-centered redox responses in 70% aqueous MeCN (Table 3). This solvent mixture was necessary for sufficient solubility of all compounds in the same medium. All the Zn^{II} complexes demonstrated two-electron, irreversible reductions at very low potentials (less than −1400 mV *vs* NHE) and can be considered effectively redox-inert in a biological context. In addition to the $Fe^{III/II}$ electrochemistry reported before,[2] we obtained $Mn^{III/II}$, $Co^{III/II}$, $Ni^{III/II}$, and $Cu^{II/I}$ redox couples. In the majority of cases, the redox couples were reversible or quasi-reversible (Table 3). In Figure 3, the cyclic voltammograms of $M(Dp44mT)_2$ (M = Mn, Fe, Co, Ni, and Cu) are assembled illustrating the variations in redox potentials.

Of most interest are the Fe and Cu complexes whose redox potentials lie within a range accessible to cellular oxidants and reductants. We have previously reported the electrochemistry of the $Fe(DpT)_2$ analogues,[2,16] and these data are included here for comparison. The $Co^{III/II}$ potentials of all complexes are very

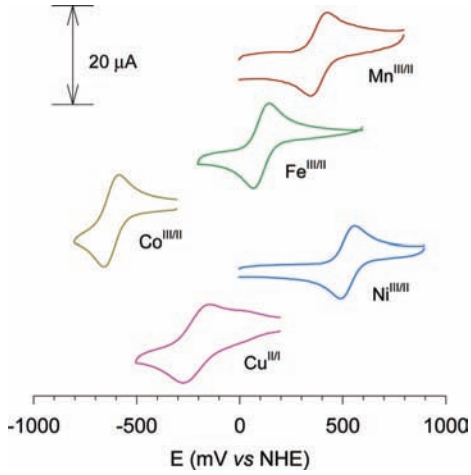

Figure 3. Cyclic voltammetry of the M(Dp44mT)$_2$ complexes (M = Mn, Fe, Co, Ni, and Cu): solvent, 70% aqueous MeCN and 0.1 M Et_4NClO_4; 100 mV s^{-1} sweep rate; glassy carbon working electrode.

Table 4. Proton-Dependent Formation Constants (log β_2*) for the **H**DpT Analogue Divalent Complexes at pH 7.4 for the Reaction $M^{2+} + 2HL \rightarrow ML_2 + 2H^+$

	$Mn^{II}L_2$	$Ni^{II}L_2$	$Cu^{II}L_2$	$Zn^{II}L_2$
HDpT	7.36	11.29	12.16	10.37
HDp4mT	7.00	11.11	12.43	10.46
HDp4eT	7.20	11.13	12.58	10.27
HDp44mT	7.76	11.21	12.49	10.20
HDp4pT	7.41	11.32	12.41	10.21
HDp4aT	7.33	11.14	12.53	10.22

low, and the Co^{II} state is inaccessible in an aerobic environment. The $Mn^{III/II}$ and $Ni^{III/II}$ redox potentials are at the high end of the potential range that may be biologically relevant. Specifically, all Mn^{II} and Ni^{II} complexes of the **H**DpT analogues are stable in neutral, aerated aqueous/organic solution and require a stronger oxidant than dioxygen to reach the trivalent oxidation state. Reversibility of the $Cu^{II/I}$ redox couples was more variable across the six **H**DpT analogue complexes and perhaps reflects the greater lability of the Cu^{I} forms and their greater tendency to dissociate than that seen with the other complexes.

In all cases, the inductive effects of the substituents on the terminal N-atom of the thiosemicarbazone gave essentially the same trends in redox potential. The most strongly electron donating $-NMe_2$ group (**H**Dp44mT) tended to provide the lowest redox potential (Table 3). In contrast, the electron withdrawing −NHPh group (**H**Dp4pT) typically shifted the corresponding redox couple to higher potentials than the other compounds in its series. We previously reported a similar trend in the $Fe^{III/II}$ redox potentials of this series.[2]

Stability Constants and Metal Exchange. We have determined the conditional formation constants of the Mn, Ni, Cu, and Zn complexes at pH 7.4 by spectrophotometric competition titrations using tetradentate nitrilotriactetate (NTA^{3-}) as the competitor. The results are given in Table 4, and they follow the expected trend based on the Irving−Williams order. The Fe^{II} complexes were an exception, and their formation constants with the **H**DpT analogues could not be determined because the tetradentate NTA^{3-} ligand (log $K[Fe(NTA)]^- = 8.9$)[36] was not competitive with the Fe-coordinated thiosemicarbazone. Other ligands such as $\mathbf{H}_4$EDTA and $\mathbf{H}_5$DTPA were also ineffective.

The reason for the remarkable rise in Fe formation constant is due to a low spin electronic configuration for the Fe^{II} thiosemicarbazone complex. Complex formation constants of Fe^{II} complexes rise by several orders of magnitude upon conversion from a high spin to a low spin ground state. As an example, the first and second stepwise complex formation constants of (high spin) Fe^{II} with 2,2′-bipyridyl are similar ($\log K_1 \approx \log K_2 \approx 4$), while the third stepwise formation constant is much greater ($\log K_3 \approx 10$) because the product tris(2,2′-bipyridyl)iron(II) is low spin.[37] These results indicate that Fe^{II} must be more competitive for each **H**DpT analogue than any of the remaining divalent ions in this study. This was confirmed qualitatively by further experiments where metal exchange between the Mn^{II}, Ni^{II}, Cu^{II}, and Zn^{II} complexes in the presence of free Fe^{II} was carried out in an anaerobic box to avoid the possibility of Fe^{III} complexes being formed. The results of these experiments demonstrated in each case the appearance of distinctively blue-green solutions characteristic of the Fe^{II} thiosemicarbazone complex. However, these transmetalation reactions proceeded at varying rates depending on the metals involved (data not shown). The reverse experiment where the corresponding Fe(DpT)$_2$ analogue was incubated with Mn^{II}, Ni^{II}, Cu^{II}, or Zn^{II} gave no change in the electronic spectrum over a period of days, as expected from the inert nature of the low spin Fe^{II} thiosemicarbazone complex. In other words the equilibrium constant for the Fe^{II} transmetalation reaction was not able to be determined accurately. However, the results clearly indicate that the **H**DpT analogues exhibit a much greater affinity for Fe^{II} than the other divalent metal ions and that this may have significance in understanding their biological activity.

As previously reported, the **H**DpT complexes may be isolated in either their Fe^{II} or Fe^{III} forms. All Fe^{II} complexes undergo slow oxidation in the presence of air, and it is likely that all **H**DpT analogues when exposed to Fe will be converted to a complex of the type $[Fe^{III}(DpT)_2]^+$. Indeed, we carried out a competition experiment between one of the ligands, **H**Dp44mT, and the hexadentate Fe chelator desferrioxamine (DFO, Chart 1). DFO is known to form a highly stable Fe^{III} complex ($\log K = 31.0$)[38] and is among one of the most widely used Fe chelators in the clinic, particularly in chelation therapy for the treatment of Fe overload disorders.[39] It has also been identified as a possible anticancer drug, although its efficacy in this regard is very low.[40] Incubation of Fe(DFO) (100 μM) with a 20-fold excess of tridentate **H**Dp44mT resulted in gradual conversion to the corresponding $[Fe(Dp44mT)_2]^+$ complex. Spectra taken at different times over a 96 h period showed an increase in absorption at 390 nm due to the Fe^{III} thiosemicarbazone complex (Supporting Information Figure S2). It is clear that the thiosemicarbazones may compete effectively with DFO for Fe^{III} and are likely to also be highly competitive for Fe^{III} over divalent metals *in vivo*.

Antiproliferative Activity. The ability of each ligand and complex to inhibit the proliferation of the human leukemia HL60 cell line was examined (Table 5). The majority of the free **H**DpT ligands demonstrated potent antiproliferative activity in this cell line, with **H**Dp44mT and **H**Dp4pT showing the greatest anticancer effects ($IC_{50} = 0.01$ μM). Interestingly, the antiproliferative activities of the free ligands are greatest (lowest IC_{50}) when their partition coefficients (log P values) are approximately 2, while the more hydrophilic or hydrophobic chelators are less active. At either very low or very high log P values, the antiproliferative activity decreases significantly in each case. The more hydrophilic chelators probably are hindered from crossing cellular membranes as seen for DFO,[40] while the hydrophobic (high log P) compounds could be sequestered within membranes, again resulting in decreased antiproliferative efficacy.[41,42]

Table 5. Antiproliferative activity against HL60 human leukemia cells of the **H**DpT analogues and their complexes (expressed as IC_{50} values, μM), determined by the MTT assay over 72 h[a]

		IC_{50} (μM)							
	log *P*(**H**L)	**H**L (free ligand)	$Mn^{II}L_2$	$Fe^{II}L_2$	$[Fe^{III}L_2]^+$	$[Co^{III}L_2]^+$	$Ni^{II}L_2$	$Cu^{II}L_2$	$Zn^{II}L_2$
no chelator			*>6.25*	*>6.25*	*>6.25*	*>6.25*	*>6.25*	*>6.25*	*>6.25*
HDpT	0.78	2.2 ± 0.1	0.69 ± 0.03	*>6.25*	*>6.25*	*>6.25*	*>6.25*	2.5 ± 0.3	1.24 ± 0.05
HDp4mT	3.18	1.41 ± 0.06	0.44 ± 0.03	1.53 ± 0.5	0.5 ± 0.2	*>6.25*	1.24 ± 0.01	0.15 ± 0.01	0.44 ± 0.02
HDp4eT	1.23	0.05 ± 0.01	0.29 ± 0.01	0.38 ± 0.1	0.07 ± 0.02	4.2 ± 0.1	0.04 ± 0.02	0.03 ± 0.01	0.04 ± 0.001
HDp44mT	2.19	0.01 ± 0.001	0.01 ± 0.001	0.08 ± 0.03	0.07 ± 0.02	0.29 ± 0.03	0.01 ± 0.001	0.01 ± 0.001	0.01 ± 0.001
HDp4pT	1.96	0.01 ± 0.002	0.01 ± 0.002	0.06 ± 0.02	0.05 ± 0.01	0.22 ± 0.03	0.04 ± 0.003	0.01 ± 0.001	0.01 ± 0.002
HDp4aT	1.68	0.05 ± 0.02	0.02 ± 0.001	0.33 ± 0.05	0.4 ± 0.08	3.28 ± 0.04	0.01 ± 0.004	0.03 ± 0.01	0.02 ± 0.002

[a] Values >6.25 μM (italics) indicate an inactive compound. Experiments with no chelator were performed with the uncomplexed sulfate (Cu^{II}, Fe^{II}) or chloride (Mn^{II}, Fe^{III}, Co^{II}, Ni^{II}, and Zn^{II}) salts alone. Results are the mean ± SD (three experiments).

A key finding of this work was that the activity profiles of the **H**DpT free ligands and their corresponding Mn^{II}, Ni^{II}, Cu^{II}, and Zn^{II} complexes are barely distinguishable (Table 5). In other words, the most (or least) active complexes are those of the most (or least) active free ligands. Our previous studies with related complexes of aroylhydrazone chelators have indicated that the partition coefficients of the free ligands and those of their complexes are correlated and governed chiefly by the noncoordinating alkyl, aryl, or allyl substituents.[43]

The Co^{III} complexes are an exception and are consistently less active (or in some cases virtually inactive, e.g., for **H**DpT and **H**Dp4mT) compared with the corresponding divalent complexes and free ligand. The $[Co^{III}(DpT)_2]^+$ complexes of all six analogues examined differ in a number of important ways from the divalent $M^{II}(DpT)_2$ analogues in their physical properties. They carry a positive charge at pH 7.4, and this will render them less able to cross cell membranes by passive diffusion. Most importantly, they are substitution inert (low spin d^6 Co^{III} complexes). Finally, they cannot be reduced to their labile Co^{II} form by any known biological reductant on the basis of our electrochemical results. Even if the compounds penetrate the cell membrane, they should be both substitution and redox inert. Modest antiproliferative activity is observed for the Co^{III} complexes of **H**Dp4pT and **H**Dp44mT (Table 5), indicating other factors may contribute to the cytotoxicity of these compounds, but this is at least an order of magnitude lower activity than seen in all other corresponding divalent complexes or free ligands.

The striking parallels between the antiproliferative activity of the thiosemicarbazone free ligands and their divalent Mn, Ni, Cu, and Zn complexes (in contrast with the low activity of the substitution-inert Co^{III} complexes) suggest that the labile divalent complexes dissociate within the cell to liberate their respective free thiosemicarbazone, which is known to markedly inhibit tumor growth.[16,18] Indeed, our metal exchange experiments above showed that *in vitro* the divalent complexes undergo rapid exchange upon encountering Fe^{II} or Fe^{III}.

In a prior study, we demonstrated that both the free **H**DpT ligands and their Fe complexes (Fe^{II} and Fe^{III}) exhibit antiproliferative activity against human SK-N-MC neuroepithelioma (brain tumor) cells.[2] Similar results in the current study were obtained using the human HL60 leukemic cell line (Table 5), confirming the wide spectrum of antitumor activity of the DpT chelators.[16,18] We previously noted that complexation with Fe^{II} or Fe^{III} lowers the antiproliferative activity of the **H**DpT ligands significantly,[2] and we observe the same trend here (Table 5). It is of interest that the difference in antitumor efficacy between the Fe^{II} and Fe^{III} complexes was not marked. Considering this, it should be taken into account that the Fe^{II} complexes spontaneously oxidize in an aerobic environment, which may be occurring during the course of the antiproliferative assay (i.e., 72 h). However, most relevant to this study is the fact that the antiproliferative activity of the Fe complexes is lower by approximately an order of magnitude across the series (Table 5) than the corresponding divalent Mn, Ni, Cu and Zn complexes, which are as active as the metal-free ligands.

There are three conclusions that can be drawn from these results. First, since the Fe complexes are much less active than the divalent Mn, Ni, Cu, and Zn complexes, this could indicate that presaturation of the ligand with Fe prevents chelation of cellular Fe that is vital for a range of essential biological processes, including DNA synthesis. Second, the Fe complexes may act to donate their bound Fe to the cell to stimulate cellular proliferation, attenuating to some degree the cytotoxic effect of the released free ligand. Previous studies have shown that Fe complexes of aroylhydrazones possessing structures similar to the structures of the present thiosemicarbazones can donate Fe to cells that can then take part in physiologically relevant processes.[44,45] Third, the similarity of the biological activity of the free ligand with the corresponding divalent Mn, Ni, Cu, and Zn complexes indicates that these complexes most likely act as transport vehicles of the ligand into the cell that dissociate to liberate the free chelator, which then mediates their antiproliferative effects. Cumulatively, these results indicate that the dissociation of the labile divalent Mn, Ni, Cu, and Zn complexes of the **H**DpT series within the cell and subsequent chelation of Fe by the free ligand may play a role in their potent antitumor activity. A previous investigation in our laboratory[23] examined the antiproliferative activity of the Mn, Co, Fe, Zn, Ni, and Cu complexes of the **H**PKIH series of ligands (Chart 1). For some of these complexes, particularly those of **H**PKBH,[23] all of the complexes showed significantly greater antiproliferative activity than the free ligand alone. However, for these latter compounds, the antitumor activity of the hydrazone ligands[23] was lower by orders of magnitude compared with the present **H**DpT thiosemicarbazones. In the case of the hydrazone ligands, the cytotoxic effects of the donated free metal ion could have been more significant than that of the free chelators.

Conclusions

The **H**DpT series of ligands hold much potential as novel chemotherapeutics for cancer treatment. The work performed in this study adds to our understanding of the mechanism of action of these promising agents. Specifically, we synthesized Mn^{II}, Co^{III}, Ni^{II}, Cu^{II}, and Zn^{II} complexes and examined their antiproliferative activity in comparison to their corresponding free ligands and $Fe^{III/II}$ complexes. Only the Cu^{II} and $Fe^{III/II}$ complexes were found to be redox active at potentials available to cellular oxidants and reductants, which may play a role in their biological activity. Significantly, the divalent Mn, Ni, Cu, and Zn complexes were observed to have the same high antiproliferative activity as the free ligand. This suggests a

transmetalation mechanism, where the labile complex dissociates intracellularly to yield the free ligand with subsequent binding of essential Fe.

Experimental Procedures

Syntheses. Precursors. The free ligands were prepared and characterized as described previously[2] by condensation of di-2-pyridylketone with the appropriate thiosemicarbazide. The Fe complexes studied in this work were also prepared according to published procedures.[2] Desferrioxamine B as its mesylate salt (DFO) was obtained commercially, and its ferric complex (Fe(DFO)) was prepared by modification of a published procedure.[46] DFO mesylate (0.328 g, 0.5 mmol) was dissolved in water (7 mL) with stirring. A freshly prepared solution of $Fe(ClO_4)_3 \cdot 6H_2O$ (0.236 g, 0.51 mmol) in $HClO_4$ (0.5 mL, 0.1 M) was added to the DFO solution. The ensuing red solution was neutralized to pH 7 with dilute NaOH and then filtered through a 0.2 μm Supor membrane filter. This solution was diluted volumetrically to 25 mL to give a ~20 mM stock solution. A 100 μM solution of ferrioxamine B was prepared by dilution of this stock solution in 10 mM MOPS buffer (pH 7.4) containing 0.1 M Et_4NClO_4. The solution was again filtered through a 0.2 μm membrane filter immediately prior to use.

Synthesis of ML_2 Complexes. All complexes were prepared by the following general method. The appropriate thiosemicarbazone (1 mmol) was dissolved in EtOH (15 mL), and Et_3N (0.37 g, 5 mmol) was added to the solution. To this mixture was added 5 mmol of the appropriate salt $M(ClO_4)_2 \cdot 6H_2O$ (M = Mn, Co, Ni, Cu, and Zn) and the mixture refluxed for 30 min. Upon cooling of the mixture, the product was collected by vacuum filtration and washed with EtOH and then Et_2O. Elemental analysis, NMR, IR, and UV−visible spectral data are given in the Supporting Information.

$[Mn^{II}(Dp4mT)_2] \cdot H_2O$: brown powder (yield 56%).
$[Co^{III}(Dp4mT)_2](ClO_4) \cdot 4H_2O$: brown powder (yield 67%).
$Ni^{II}(Dp4mT)_2$: dark-brown powder (yield 75%).
$[Cu^{II}(Dp4mT)_2] \cdot 4.5H_2O$: brown powder (yield 45%).
$Zn^{II}(Dp4mT)_2$: yellow powder (yield 87%).
$Mn^{II}(Dp44mT)_2$: brown powder (yield 55%).
$[Co^{III}(Dp44mT)_2](ClO_4) \cdot 1.5H_2O$: dark-brown powder (yield 62%).
$Ni^{II}(Dp44mT)_2$: brown powder (yield 56%).
$Cu^{II}(Dp44mT)_2$: brown powder (yield 71%).
$Zn^{II}(Dp44mT)_2$: yellow powder (yield 85%).
$[Mn^{II}(Dp4aT)_2] \cdot 1.5H_2O$: brown powder (yield 66%).
$[Co^{III}(Dp4aT)_2](ClO_4) \cdot 3H_2O$: dark-brown powder (yield 43%).
$Ni^{II}(Dp4aT)_2$: brown powder (yield 69%).
$[Cu^{II}(Dp4aT)_2] \cdot 5H_2O$: brown powder (yield 67%).
$[Zn^{II}(Dp4aT)_2] \cdot 1.5H_2O$: yellow powder (yield 89%).
$[Mn^{II}(Dp4pT)_2] \cdot 2H_2O$: brown powder (yield 57%).
$[Co^{III}(Dp4pT)_2]ClO_4$: dark-brown powder (yield 51%).
$[Ni^{II}(Dp4pT)_2] \cdot H_2O$: brown powder (yield 62%).
$[Cu^{II}(Dp4pT)_2] \cdot 0.5H_2O$: brown powder (yield 56%).
$[Zn^{II}(Dp4pT)_2] \cdot 1.5H_2O$: yellow powder (yield is 78%).
$Mn^{II}(DpT)_2$: brown powder (yield 72%).
$[Co^{III}(DpT)_2]ClO_4$: dark-brown powder (yield 45%).
$Ni^{II}(DpT)_2$: brown powder, (yield 57%).
$Cu^{II}(DpT)_2$: brown powder (yield 52%).
$Zn^{II}(DpT)_2$: yellow powder (yield 75%).
$[Mn^{II}(Dp4eT)_2] \cdot 2.5H_2O$: brown powder (yield 65%).
$[Co^{III}(Dp4eT)_2](ClO_4) \cdot 2H_2O$: dark-brown powder (yield 60%).
$Ni^{II}(Dp4eT)_2$: brown powder (yield 59%).
$Cu^{II}(Dp4eT)_2$: brown powder (yield 79%).
$Zn^{II}(Dp4eT)_2$: yellow powder (yield 78%).

Physical Methods. Solution UV−visible spectra were measured on an Analytikjena Specord 210 UV−visible spectrophotometer for work on the bench or a Shimadzu UV-Mini instrument housed within a Belle Technology anaerobic box for work under an inert atmosphere (O_2 < 10 ppm). Infrared spectra were measured on a Perkin-Elmer model 1600 FT-IR spectrophotometer with an ATR attachment. ^1H and ^{13}C NMR spectra were acquired on a Bruker AV400 spectrometer using DMSO-d_6 as solvent. Electron paramagnetic resonance (EPR) spectra were measured on a Bruker ER200 instrument at Q-band frequency (~9.3 GHz) in 1 mM 1:2 H_2O/DMF frozen solutions at 77 K. Spectra were simulated with the program EasySpin.[47] All simulated spectra and their spin Hamiltonian parameters appear in the Supporting Information (Figure S1).

Cyclic voltammetry was performed with a BAS100B/W potentiostat employing a glassy carbon working electrode, a platinum auxiliary electrode, and an aqueous Ag/AgCl reference electrode (E^o = 196 mV *vs* NHE). Concentrations of complexes were 1−5 mM, and 0.1 M Et_4NClO_4 was the supporting electrolyte in 70% aqueous MeCN. The use of this solvent was necessary because of the low solubility of the compounds in water alone.

Stability Constant Determinations. The conditional stability constants of the Mn^{II}, Ni^{II}, Cu^{II}, and Zn^{II} complexes were determined by a spectrophotometric competition titration with nitrilotriacetic acid (H_3NTA). Metal stock solutions of the appropriate $M(ClO_4)_2 \cdot 6H_2O$ (M = Ni, Cu, Zn) salt were prepared using Milli-Q water containing 10 mM MOPS buffer and 0.1 M Et_4NClO_4, and the pH was adjusted to 7.4 using Et_4NOH solution. Accurate metal ion concentrations were determined by inductively coupled plasma mass spectrometry (Analytical Services Unit, School of Land and Food Sciences, University of Queensland). Stock solutions of each thiosemicarbazone were prepared fresh daily by dissolving a known amount of ligand in DMSO. Metal/thiosemicarbazone solutions were prepared by addition of a known volume of metal stock solution and ligand solution (approximately 1 mL), which was diluted accurately to 100 mL with MOPS buffer solution, to give a final solution of ~10 μM in metal ion and 30 μM in ligand. The ligand was used in excess to suppress metal hydrolysis. A 150 μM NTA^{3-} solution was prepared in the same buffer. A 10 mL aliquot of metal/thiosemicarbazone solution was titrated with 20 sequential 0.5 mL aliquots of NTA solution. The solution was mixed thoroughly between each addition. A small volume was withdrawn, and its UV−visible spectrum was measured before being returned to the titration solution. UV−visible spectra in the range 200−450 nm were acquired after each addition. Each titration was performed in triplicate. Proton-dependent stability constants were determined using the computer program, Specfit (version 3.0.40).[48] The model used assumed formation of both ML and ML_2 thiosemicarbazone complexes. The stability constants for the 1:1 metal/NTA complexes were taken from the NIST Critical Stability Constant database.[36] The stability constants of the metal/thiosemicarbazone complexes are given in Table 4. Metal exchange reactions between the divalent complexes and Fe^{II} were carried out within a Belle Technology anaerobic box (O_2 < 10 ppm) to avoid oxidation to their Fe^{III} analogues.

Crystallography. For $[Mn(Dp4pT)_2] \cdot$DMF, $Cu(Dp44mT)_2$, and $Zn(Dp4mT)_2$ (each crystallized from aqueous DMF) cell constants were determined by a least-squares fit to the setting parameters of 25 independent reflections measured on an Enraf-Nonius CAD4 four circle diffractometer. Crystallographic data for $[Fe(DpT)_2]ClO_4$ and $[Ni(Dp4pT)_2] \cdot {}^1/_2MeCN \cdot {}^1/_2H_2O$ (each crystallized from aqueous MeCN) were collected on an Oxford Diffraction Gemini Ultra S CCD diffractometer. Graphite monochromated Mo Kα radiation (0.710 73 Å) was used in each case, and data were collected in the range $2° < 2\theta < 50°$. Data reduction and absorption corrections were performed within WINGX[49] for data collected on the CAD4 diffractometer and CrysAlisPro (Oxford Diffraction, version 171.32.15) for data collected on the Gemini CCD instrument. All structures were solved by direct methods with SHELXS-86 and refined by full-matrix least-squares analysis against F^2 with SHELXL-97.[50] H atoms were included at estimated positions. Drawings of molecules were produced with ORTEP3.[51] Crystal data are summarized in Table 1. All data have been deposited with the Cambridge Crystallographic Data Centre in CIF format (CCDC 698207−698211).

Biological Studies. Cell Culture. The HL60 human leukemia cell line was a kind gift from Dr. Christopher R. Chitambar (Division of Neoplastic Disease, Medical College of Wisconsin, Milwaukee, WI), and cells were grown as previously described.[52]

Briefly, HL60 cells were grown in RPMI (Invitrogen, Mt. Waverly, VIC, Australia) containing 10% fetal bovine serum, 100 μg/mL streptomycin (Invitrogen), 100 U/mL penicillin (Invitrogen), 1% nonessential amino acids (Invitrogen), and 0.28 μg/mL fungizone (Squibb Pharmaceuticals, Montreal, QC, Canada). These cells were grown at 37 °C in a humidified atmosphere of 5% CO_2/95% air in an incubator (Forma Scientific, Marietta, OH).

Effect of the Chelators and Complexes on Cellular Proliferation. The effects of the chelators and complexes on cellular proliferation were determined by the MTT [1-(4,5-dimethylthiazol-2-yl)-2,5-diphenyltetrazolium] assay using standard techniques.[4,15] The human leukemia cell line, HL60, was seeded in 96-well microtiter plates at 1.5×10^4 cells/well in medium containing human diferric transferrin (Tf, 1.25 μM) and chelators or complexes at a range of concentrations (0−6.25 μM). Control samples contained medium with Tf (1.25 μM) without the ligands. The cells were incubated at 37 °C in a humidified atmosphere containing 5% CO_2 and 95% air for 72 h. After incubation, 10 μL of MTT (5 mg/mL) was added to each well and further incubated at 37 °C for 2 h. After solubilization of the cells with 100 μL of 10% SDS−50% isobutanol in 0.01 M HCl, the plates were read at 570 nm using a scanning multiwell spectrophotometer. The results, which are the mean values of three experiments, are expressed as a percentage of the control. The inhibitory concentration (IC_{50}) was defined as the chelator or complex concentration necessary to reduce the absorbance to 50% of the untreated control. By use of this method, absorbance was shown to be directly proportional to cell counts, as shown previously.[15]

Statistical Analysis. Experimental data were compared using Student's *t*-test. Results were expressed as the mean or mean ± SD (number of experiments) and considered to be statistically significant when $p < 0.05$.

Acknowledgment. P.V.B. and D.R.R. acknowledge the award of an Australian Research Council Discovery Grant DP0773027. D.R.R. thanks the National Health and Medical Research Council of Australia for grant and fellowship support. D.B.L. thanks the Cancer Institute NSW for fellowship support. We thank Dr. J. Howard for technical assistance with some of the biological studies reported herein.

Supporting Information Available: Elemental analysis results, NMR, IR, and UV−visible spectral data, Cu^{II} EPR spectra, and electronic difference spectra for the reaction between Fe(DFO) and **H**Dp44mT. This material is available free of charge via the Internet at http://pubs.acs.org.

References

(1) Bernhardt, P. V.; Caldwell, L. M.; Chaston, T. B.; Chin, P.; Richardson, D. R. Cytotoxic iron chelators: characterization of the structure, solution chemistry and redox activity of ligands and iron complexes of the di-2-pyridyl ketone isonicotinoyl hydrazone (HPKIH) analogues. *J. Biol. Inorg. Chem.* **2003**, *8*, 866–880.

(2) Richardson, D. R.; Sharpe, P. C.; Lovejoy, D. B.; Senaratne, D.; Kalinowski, D. S.; Islam, M.; Bernhardt, P. V. Dipyridyl thiosemicarbazone chelators with potent and selective antitumor activity form iron complexes with redox activity. *J. Med. Chem.* **2006**, *49*, 6510–6521.

(3) Kalinowski, D. S.; Sharpe, P. C.; Bernhardt, P. V.; Richardson, D. R. Design, synthesis, and characterization of new iron chelators with antiproliferative activity: structure−activity relationships of novel thiohydrazone analogues. *J. Med. Chem.* **2007**, *50*, 6212–6225.

(4) Kalinowski, D. S.; Yu, Y.; Sharpe, P. C.; Islam, M.; Liao, Y.-T.; Lovejoy, D. B.; Kumar, N.; Bernhardt, P. V.; Richardson, D. R. Design, synthesis, and characterization of novel iron chelators: structure−activity relationships of the 2-benzoylpyridine thiosemicarbazone series and their 3-nitrobenzoyl analogues as potent antitumor agents. *J. Med. Chem.* **2007**, *50*, 3716–3729.

(5) Buss, J. L.; Greene, B. T.; Turner, J.; Torti, F. M.; Torti, S. V. Iron chelators in cancer chemotherapy. *Curr. Top. Med. Chem.* **2004**, *4*, 1623–1635.

(6) Torti, S. V.; Torti, F. M.; Whitman, S. P.; Brechbiel, M. W.; Park, G.; Planalp, R. P. Tumor cell cytotoxicity of a novel metal chelator. *Blood* **1998**, *92*, 1384–1389.

(7) Rakba, N.; Loyer, P.; Gilot, D.; Delcros, J. G.; Glaise, D.; Baret, P.; Pierre, J. L.; Brissot, P.; Lescoat, G. Antiproliferative and apoptotic effects of O-Trensox, a new synthetic iron chelator, on differentiated human hepatoma cell lines. *Carcinogenesis* **2000**, *21*, 943–951.

(8) Finch, R. A.; Liu, M.; Grill, S. P.; Rose, W. C.; Loomis, R.; Vasquez, K. M.; Cheng, Y.; Sartorelli, A. C. Triapine (3-aminopyridine-2-carboxaldehyde- thiosemicarbazone): a potent inhibitor of ribonucleotide reductase activity with broad spectrum antitumor activity. *Biochem. Pharmacol.* **2000**, *59*, 983–991.

(9) Odenike, O. M.; Larson, R. A.; Gajria, D.; Dolan, M. E.; Delaney, S. M.; Karrison, T. G.; Ratain, M. J.; Stock, W. Phase I study of the ribonucleotide reductase inhibitor 3-aminopyridine-2-carboxaldehyde-thiosemicarbazone (3-AP) in combination with high dose cytarabine in patients with advanced myeloid leukemia. *Invest. New Drugs* **2008**, *26*, 233–239.

(10) Karp, J. E.; Giles, F. J.; Gojo, I.; Morris, L.; Greer, J.; Johnson, B.; Thein, M.; Sznol, M.; Low, J. A phase I study of the novel ribonucleotide reductase inhibitor 3-aminopyridine-2-carboxaldehyde thiosemicarbazone (3-AP, Triapine) in combination with the nucleoside analog fludarabine for patients with refractory acute leukemias and aggressive myeloproliferative disorders. *Leuk. Res.* **2008**, *32*, 71–77.

(11) Richardson, D. R. Molecular mechanisms of iron uptake by cells and the use of iron chelators for the treatment of cancer. *Curr. Med. Chem.* **2005**, *12*, 2711–2729.

(12) Kalinowski, D. S.; Richardson, D. R. The evolution of iron chelators for the treatment of iron overload disease and cancer. *Pharmacol. Rev.* **2005**, *57*, 547–583.

(13) Nurtjahja-Tjendraputra, E.; Fu, D.; Phang, J.; Richardson, D. R. Iron chelation regulates cyclin D1 expression via the proteasome: a link to iron-deficiency mediated growth suppression. *Blood* **2007**, *109*, 4045–4054.

(14) Fu, D.; Richardson, D. R. Iron chelation and regulation of the cell cycle: two mechanisms of post-transcriptional regulation of the universal cyclin-dependent kinase inhibitor p21CIP1/WAF1 by iron-depletion. *Blood* **2007**, *110*, 752–761.

(15) Richardson, D. R.; Tran, E. H.; Ponka, P. The potential of iron chelators of the pyridoxal isonicotinoyl hydrazone class as effective antiproliferative agents. *Blood* **1995**, *86*, 4295–4306.

(16) Yuan, J.; Lovejoy, D. B.; Richardson, D. R. Novel di-2-pyridyl-derived iron chelators with marked and selective antitumor activity: in vitro and in vivo assessment. *Blood* **2004**, *104*, 1450–1458.

(17) Richardson, D. R.; Bernhardt, P. V. Crystal and molecular structure of 2-hydroxy-1-naphthaldehyde isonicotinoyl hydrazone (NIH) and its iron(III) complex: an iron chelator with anti-tumor activity. *J. Biol. Inorg. Chem.* **1999**, *4*, 266–273.

(18) Whitnall, M.; Howard, J.; Ponka, P.; Richardson, D. R. A class of iron chelators with a wide spectrum of potent anti-tumor activity that overcome resistance to chemotherapeutics. *Proc. Natl. Acad. Sci. U.S.A.* **2006**, *103*, 14901–14906.

(19) Armstrong, C. M.; Bernhardt, P. V.; Chin, P.; Richardson, D. R. Structural variations and formation constants of first-row transition metal complexes of biologically active aroylhydrazones. *Eur. J. Inorg. Chem.* **2003**, *114*, 5–1156.

(20) Bernhardt, P. V.; Chin, P.; Sharpe, P. C.; Richardson, D. R. Hydrazone chelators for the treatment of iron overload disorders: iron coordination chemistry and biological activity. *Dalton Trans.* **2007**, 3232–3244.

(21) Bernhardt, P. V.; Wilson, G. J.; Sharpe, P. C.; Kalinowski, D. S.; Richardson, D. R. Tuning the antiproliferative activity of biologically active iron chelators: characterization of the coordination chemistry and biological efficacy of 2-acetylpyridine and 2-benzoylpyridine hydrazone ligands. *J. Biol. Inorg. Chem.* **2008**, *13*, 107–119.

(22) Kalinowski, D. S.; Richardson, D. R. Iron chelators and differing modes of action and toxicity: the changing face of iron chelation therapy. *Chem. Res. Toxicol.* **2007**, *20*, 715–720.

(23) Bernhardt, P. V.; Mattsson, J.; Richardson, D. R. Complexes of cytotoxic chelators from the dipyridyl ketone isonicotinoyl hydrazone (HPKIH) analogues. *Inorg. Chem.* **2006**, *45*, 752–760.

(24) Philip, V.; Suni, V.; Kurup, M. R. P.; Nethaji, M. Manganese(II) complexes of substituted di-2-pyridyl ketone thiosemicarbazones: structural and spectral studies. *Spectrochim. Acta, Part A* **2006**, *64*, 171–177.

(25) Suni, V.; Kurup, M. R. P.; Nethaji, M. Structural and spectral investigations on some new Ni(II) complexes of di-2-pyridyl ketone *N*(4)-phenylthiosemicarbazone. *Polyhedron* **2007**, *26*, 3097–3102.

(26) Irving, H.; Williams, R. J. P. Order of stability of metal complexes. *Nature* **1948**, *162*, 746–747.

(27) Garcia-Tojal, J.; Pizarro, J. L.; Lezama, L.; Arriortua, M. I.; Rojo, T. Spectroscopic and magnetic properties of the pyridine-2-carbaldehyde thiosemicarbazonateiron(III) complexes: $[Fe(C_7H_7N_4S)_2]X \cdot nH_2O$ (X = Cl, ClO_4, NO_3, PF_6). Crystal structure of the hexafluorophosphate compound. *Inorg. Chim. Acta* **1998**, *278*, 150–158.

(28) West, D. X.; Swearingen, J. K.; Valdes-Martinez, J.; Hernandez-Ortega, S.; El-Sawaf, A. K.; van Meurs, F.; Castineiras, A.; Garcia, I.; Bermejo,

E. Spectral and structural studies of iron(III), cobalt(II,III), and nickel(II) complexes of 2-pyridineformamide *N*(4)-methylthiosemicarbazone. *Polyhedron* **1999**, *18*, 2919–2929.
(29) Sreekanth, A.; Kurup, M. R. P. Synthesis, EPR and Moessbauer spectral studies of new iron(III) complexes with 2-benzoylpyridine-*N*(4),*N*(4)-(butane-1,4-diyl) thiosemicarbazone (HBpypTsc): X-ray structure of $[Fe(BpypTsc)_2]FeCl_4 \cdot 2H_2O$ and the free ligand. *Polyhedron* **2004**, *23*, 969–978.
(30) Sreekanth, A.; Fun, H.-K.; Kurup, M. R. P. Structural and spectral studies of an iron(III) complex $[Fe(Pranthas)_2][FeCl_4]$ derived from 2-acetylpyridine-*N*(4),*N*(4)-(butane-1,4-diyl) thiosemicarbazone (HPranthas). *J. Mol. Struct.* **2005**, *737*, 61–67.
(31) Duan, C.-Y.; Wu, B.-M.; Mak, T. C. W. Synthesis and structural characterization of the new quadridentate N_3S-compound di-2-pyridyl ketone thiosemicarbazone and its binuclear copper(II) complexes. *J. Chem. Soc., Dalton Trans.* **1996**, 3485–3490.
(32) Duan, C.-Y.; You, X.-Z.; Mak, T. C. W. Bis[μ-(di-2-pyridyl ketone thiosemicarbazonato-N1,N′′,S:N′)]bis[(acetato-O)copper(II)] dimethanol solvate. *Acta Crystallogr., Sect. C* **1998**, *54*, 1397–1399.
(33) Duan, C.-Y.; You, X.-Z.; Mak, T. C. W. Bis[μ-(di-2-pyridyl ketone thiosemicarbazonato-N1,N′′,S:N′)]bis[(isothiocyanaato-N)copper(II)] bis(dimethylformamide) solvate. *Acta Crystallogr., Sect. C* **1998**, *54*, 1395–1397.
(34) Philip, V.; Suni, V.; Kurup, M. R. P.; Nethaji, M. Novel binuclear copper(II) complexes of di-2-pyridyl ketone *N*(4)-methyl, *N*(4)-phenylthiosemicarbazone: structural and spectral investigations. *Polyhedron* **2005**, *24*, 1133–1142.
(35) Philip, V.; Suni, V.; Prathapachandra Kurup, M. R.; Nethaji, M. Copper(II) complexes derived from di-2-pyridyl ketone *N*(4),*N*(4)-(butane-1,4-diyl)thiosemicarbazone: crystal structure and spectral studies. *Polyhedron* **2006**, *25*, 1931–1938.
(36) Martell, A. E.; Smith, R. M.; Motekaitis, R. J. *NIST Critically Selected Stability Constants of Metal Complexes*, version 8.0; NIST: Gaithersburg, MD, 2004.
(37) Irving, H.; Mellor, D. H. Stability of metal complexes of 1,10-phenanthroline and its analogs. I. 1,10-Phenanthroline and 2,2′-bipyridine. *J. Chem. Soc.* **1962**, 5222–5237.
(38) Raymond, K. N.; Carrano, C. J. Coordination chemistry and microbial iron transport. *Acc. Chem. Res.* **1979**, *12*, 183–190.
(39) Bernhardt, P. V. Coordination chemisstry and biology of chelators for the treatment of iron overload disorders. *Dalton Trans.* **2007**, 3214–3220.
(40) Richardson, D. R.; Ponkas, P.; Baker, E. The effect of the iron(III) chelator, desferrioxamine, on iron and transferrin uptake by the human malignant melanoma cell. *Cancer Res.* **1994**, *54*, 685–689.
(41) Baker, E.; Page, M.; Torrance, J.; Grady, R. W. Effect of desferrioxamine, rhodotorulic acid and cholylhydroxamic acid on transferrin and iron exchange with hepatocytes in culture. *Clin. Physiol. Biochem.* **1985**, *3*, 277–288.
(42) Opletalová, V.; Kalinowski, D. S.; Vejsová, M.; Kuneš, J.; Pour, M.; Jampílek, J.; Buchta, V.; Richardson, D. R. Identification and characterization of thiosemicarbazones with anti-fungal and anti-tumor effects: cellular iron-chelation mediating cytotoxic activity. *Chem. Res. Toxicol.* **2008**, *21*, 1878–1889.
(43) Edward, J. T.; Ponka, P.; Richardson, D. R. Lipophilicity of the ligands and iron(III) complexes of analogues of pyridoxal isonicotinoyl hydrazone. Relationship to biological activity. *BioMetals* **1995**, *8*, 209–217.
(44) Ponka, P.; Schulman, H. M.; Wilczynska, A. Ferric pyridoxal isonicotinoyl hydrazone can provide iron for heme synthesis in reticulocytes. *Biochim. Biophys. Acta* **1982**, *718*, 151–156.
(45) Ponka, P.; Schulman, H. M. Acquisition of iron from transferrin regulates reticulocyte heme synthesis. *J. Biol. Chem.* **1985**, *260*, 14717–14721.
(46) Muetterties, K. A.; Hoener, B. A.; Engelstad, B. L.; Tongol, J. M.; Wikstrom, M. G.; Wang, S. C.; Eason, R. G.; Moseley, M. E.; White, D. L. Ferrioxamine B derivatives as hepatobiliary contrast agents for magnetic resonance imaging. *Magn. Reson. Med.* **1991**, *22*, 88–100.
(47) Stoll, S.; Schweiger, A. EasySpin, a comprehensive software package for spectral simulation and analysis in EPR. *J. Magn. Reson.* **2006**, *178*, 42–55.
(48) Binstead, R. A. *SPECFIT. Global Analysis System*; Spectrum Software Associates: Marlborough, MA, 2007.
(49) Farrugia, L. J. WINGX. *J. Appl. Crystallogr.* **1999**, *32*, 837.
(50) Sheldrick, G. M. *SHELX97. Programs for Crystal Structure Analysis*, release 97-2; University of Göttingen: Göttingen, Germany, 1998.
(51) Farrugia, L. J. ORTEP-3 for Windows, a version of ORTEP-III with a graphical user interface. *J. Appl. Crystallogr.* **1997**, *30*, 565.
(52) Davies, N. P.; Rahmanto, Y. S.; Chitambar, C. R.; Richardson, D. R. Resistance to the antineoplastic agent gallium nitrate results in marked alterations in intracellular iron and gallium trafficking: identification of novel intermediates. *J. Pharmacol. Exp. Ther.* **2006**, *317*, 153–162.

JM801012Z